A Macro-Element Approach for Non-linear Response of Offshore Skirted Footings

Barari, Amin; Ibsen, Lars Bo

Citation for published version (APA):
Barari, A., & Ibsen, L. B. (2018). A Macro-Element Approach for Non-linear Response of Offshore Skirted
Footings. In H. Khabbaz, H. Youn, & M. Bouassida (Eds.), New Prospects in Geotechnical Engineering Aspects
of Civil Infrastructures: Proceedings of the 5th GeoChina International Conference 2018 – Civil Infrastructures
Confronting Severe Weathers and Climate Changes: From Failure to Sustainability, held on July 23 to 25, 2018
in HangZhou, China (pp. 127-139). Article SUCI-D-17-00230 Springer. https://doi.org/10.1007/978-3-319-95771-
5_11

A Macro-Element Approach for Non-linear Response of Offshore Skirted Footings

Amin Barari[1], A.M. ASCE and Lars Bo Ibsen[2], M. ASCE

[1]Postdoc, Department of Civil and Environmental Engineering, Virginia Tech, 200 Patton Hall, Blacksburg, Virginia, USA, abarari@vt.edu.
[2]Pofessor, Department of Civil Engineering, Aalborg University, Thomas Manns Vej 23, 9220 Aalborg Ø, Denmark.

ABSTRACT: In recent times, shallow foundations have become more diverse, and now include concrete or steel bucket foundations used as anchors for floating platforms or as foundation for offshore wind turbines. They are always subjected to significant cyclic lateral loads due to wind and wave action.
A work-hardening plasticity model for the moment and horizontal force resultants associated with the displacements of the offshore suction caissons is herein developed. In addition, in order to better understand the performance of offshore bucket foundations under cyclic lateral loads series of cyclic lateral load tests were carried out on small scale models in a special rig developed for the cyclic tests at Aalborg University. The influence of cyclic lateral loads on the bucket lateral secant stiffness is investigated and a function is utilized to investigate it due to permanent displacements. The bucket stiffness increased with number of cycles irrespective of the load characteristics which contradicts the traditional solutions to tackle this complex situation.

INTRODUCTION

Political, industrial and technological drivers are promoting the development of offshore wind farms. Offshore wind turbines are steadily increasing in terms of size. The offshore location of these viable solutions is preferred due to its intrinsic merits to alleviate the noise, size and vibrations effects on human activities (Bhattacharya and Adhikari 2011). Suction caisson foundation is an option that can decrease the overall cost and increase the diffusion of the wind turbine. The horizontal load divided by the vertical load for the bucket foundations in wind turbines is very high compared with the suction caissons for offshore oil and gas industry. For example, the non-dimensional quantity to represent the vertical load, $V / \gamma' d^3$ (i.e., γ' is the soil effective unit weight) is between 0.5 and 0.8 which is substantially lower than typical value of 3.5 for offshore oil industry.

The resistance observed from lateral load on suction caissons is of importance in the design of marine structures which may be subjected to the earthquakes and wave action. The difficulties with respect to the logistics and cost causes a few small-scale load tests results are available that examine the bearing capacity and deformations developed in suction bucket foundations for wind turbines (Fig.1) (Ibsen et al. 2014a, 2014b; Barari and Ibsen 2012, 2014; Larsen et al. 2013). Nevertheless, the results from these tests indicate that the combined capacity of buckets can be described in terms of kinematic mechanisms accompanying pre-failure and failure states (Ibsen et al. 2015).

Traditionally, foundations are thought to exhibit the soil- foundation stiffness reduction (API 1993). This reduction in lateral resistance depends on various conditions such as, depth of sandy soil, ratio of excess pore pressure, loading frequency, etc.

In addition, previous studies revealed that the dynamic characteristic of a wind turbine system including its natural frequency and dynamic stiffness change with either few cycles of large amplitude or millions of cycles with intermediate amplitude (Cox et al. 2011).

Recommended by Limit State Design philosophy, the design stages for a shallow foundation system during life of the structures are as follows (Arany et al. 2017):

1. Ultimate Limit state (ULS): The first step in design of offshore foundations is to estimate the capacity under in-service VHM general loading.
2. Serviceability limit state: This requires the prediction of short and long-term deformations, and the influence of cycling loading.

To date there has been no verified long-term observation of alteration of the bucket foundations stiffness. The current study summarizes the findings from a series of small-scale tests of suction caissons. The focus of this research is on dynamic characteristics of these structures. Prior to cyclic behavior, 3-D finite element analyses are presented to outline a "macro-element" model based on work-hardening plasticity theory for ULS soil-foundation interaction relevant to offshore platforms.


FIG. 1. Suction bucket foundation in Horns Rev 2 Mobile Met Mast Project

DYNAMIC CONSIDERATIONS

These structures can be described by a mathematical model where the foundation is modeled by translational and rotational springs. The stiff nature of bucket lid simplifies bucket to a rigid foundation with six degrees of freedom. For each particular harmonic excitation, the dynamic stiffness K is defined as the ratio between force (or moment) R and the displacement (or rotation) U. The impedances are defined as: two horizontal and longitudinal impedances resulting from force-displacement ratio, two rocking impedances resulting from moment-rotation ratio and one vertical resulting from a ratio between harmonic vertical force and harmonic vertical displacement of the soil-foundation interface. Similarly the tensional impedance is defined from moment moment-rotation ratio about the vertical axis (z).

STATIC BEHAVIOUR OF SUCTION BUCKET: NUMERICAL MODELING

A three-dimensional finite element model using the program system PLAXIS was utilized to simulate the behavior of a laterally loaded bucket foundations. Sub-soil and bucket were modeled using the full-mesh system. A schematic view of bucket under horizontal loading is shown in Figure 2.
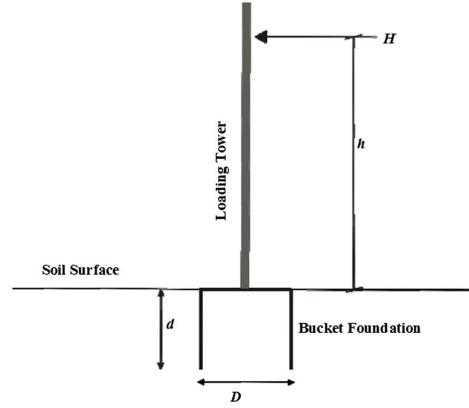
**FIG. 2. A schematic view of bucket under horizontal loading**

A bucket foundation supporting a 10 MN wind turbine, with $D = 12$ m and $d/D = 0.75$, withstanding a wave load with arm from the soil surface, h = 0.2D, 1.66D and 8.33D, and installed in very dense sand, is taken as real-scale model. The discredited model area had at least 6 times the bucket diameter. The bottom boundary of the model was extended twice the skirt length below the toe of the bucket. A typical mesh of the finite element model with geometrical properties is depicted in Figure 3.

The elasto-plastic material law with Mohr-Coulomb failure criterion was used when extended by a stress-dependency of the oedometer stiffness with the following equation (EAU 2004; Kuo et al. 2012):

$$E_S = \kappa \sigma_{at} \left(\frac{\sigma_m}{\sigma_{at}} \right)^{\lambda} \tag{1}$$

Herein $\sigma_{at} = 100 \, kN \, / \, m^2$ is a reference stress and σ_m is the current mean principle stress. The parameters κ and λ correspond to the soil stiffness at the reference stress state and stress dependency of the soil stiffness, respectively.
The input-model parameters for the dense sand are reported in Table 1.
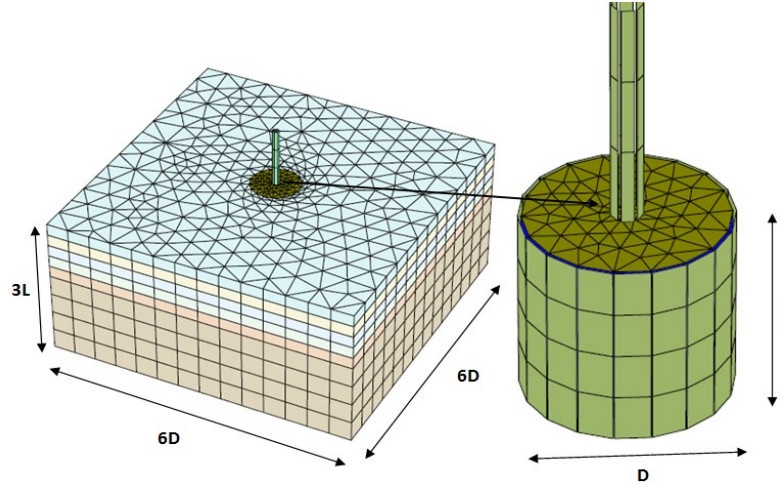
FIG. 3. Finite element model of a suction caisson system

Accordingly, the results of FE analyses offer the opportunity to compare the force-displacement curves which are of special interest for design of wind turbines, to those already reported in the literature (Fig. 4).
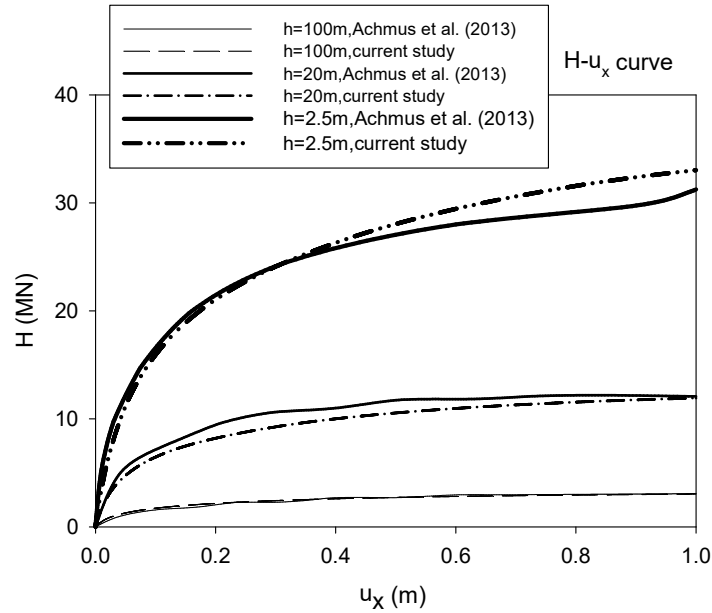
FIG. 4. Load-deformation curves for suction caisson foundations in dense sand

Table 1. Soil parameters considered (Achmus et al.2013)

Property	Value	Unit
Buoyant unit weight (γ')	11	[kN/m³]
Oedometer stiffness parameter (κ)	600	[-]
Oedometer stiffness parameter (λ)	0.55	[-]
Poisson's ratio (ν)	0.25	[-]
Internal friction angle (φ')	40	[º]
Dilation angle (ψ)	10	[º]
Cohesion (C')	0.1	[kN/m²]

Failure Envelopes: Macro-Element Approach

Macro-element modeling is applicable to many kinds of geotechnical problems but its primary application is on shallow foundations.

Given a shallow footing, model consists of structure, surrounding soil and displacement or load field applied to the system. For shallow foundations, the concept has perhaps its origin with Roscoe and Schofield (1957).

A series of FE calculations are presented herein to deduce the failure envelopes in H-M space, following a strain-hardening plasticity framework. The new model is made by giving emphasis on the relationship of applied displacement and corresponding load in yield/plastic failure state.

Figure 5 depicts representative data calculated for varying embedment ratio, L/D. The applied horizontal load, H and overturning moment, M are normalized with the associated ultimate capacities.

Given the parabolic behavior of failure envelope, the following oblique parabolic expression is adopted for offshore shallow footings to fit the numerical results:

$$f = \left(\frac{H}{H_u}\right)^2 + \left(\frac{M}{M_u}\right)^2 + n_3 \left(\frac{H}{H_u}\right)\left(\frac{M}{M_u}\right) - 1 = 0 \tag{2}$$

where n_3 is a parameter controlling the shape of surface (Gerolymos et al. 2012)

A normalized presentation of the results was also sought for the effect of n^3 on shape of normalized failure envelopes in Figure 6. As a result, the shape of normalized failure envelopes remains identical for embedment ratios $L/D \geq 0.75$.
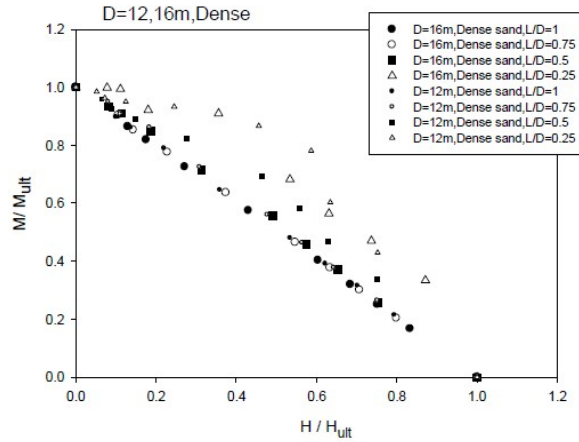
FIG.5. H-M failure envelope normalized by corresponding pure capacities at V=0
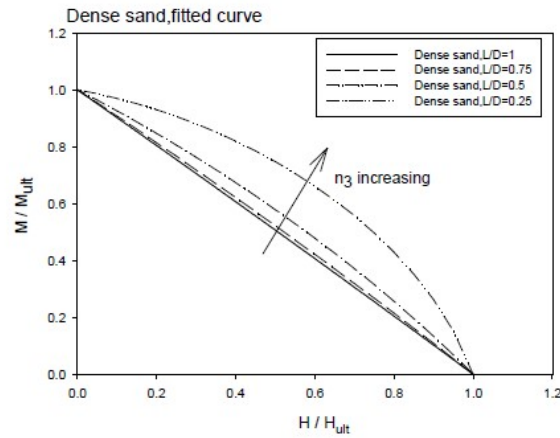
FIG. 6. Contraction of normalized yield envelopes with increasing n_3

## PERFORMANCE MEASURE PARAMETERS FOR SUCTION BUCKET SYSTEMS

Test Equipment and Program

A loading rig is utilized to apply cyclic loading which is outlined in Figure 7. The rig consists of a soil container $(1.6 \times 1.6 \times 1.15 \ m^3)$, steel frame, weight hangers, lever arm with a driving motor. The rig was more recently described by Foglia et al. (2012) to carry out cyclic loading tests on bucket foundations installed in saturated sand. The tests were performed on a caisson of diameter D=300 mm and d/D=1. The mass of the superstructure in real-scale suction caisson-supported wind turbine is parametrically given a typical value here corresponding to a static factor of safety FS_V =2. The experimental setup and loading time histories are portrayed in Figure 7.

Tests results

In this section results of three force-controlled lateral loads conducted on the lever arm are presented. The loading time-histories were: (i) 9976 cycles from 162.4 N to -68.11 N (test C35) (ii) 10153 cycles from 203.3 N to -81.7 N (test C36) (iii) 10083 cycles from 244.4 N to -90.3 N (test C37).

All the information on the cyclic lateral load tests is listed in Table 2. Figure 8 displays lateral force-displacement hysteresis curves while displacements were measured at the load reference point as previously introduced by Butterfield et al. 1997 (Figure 9).
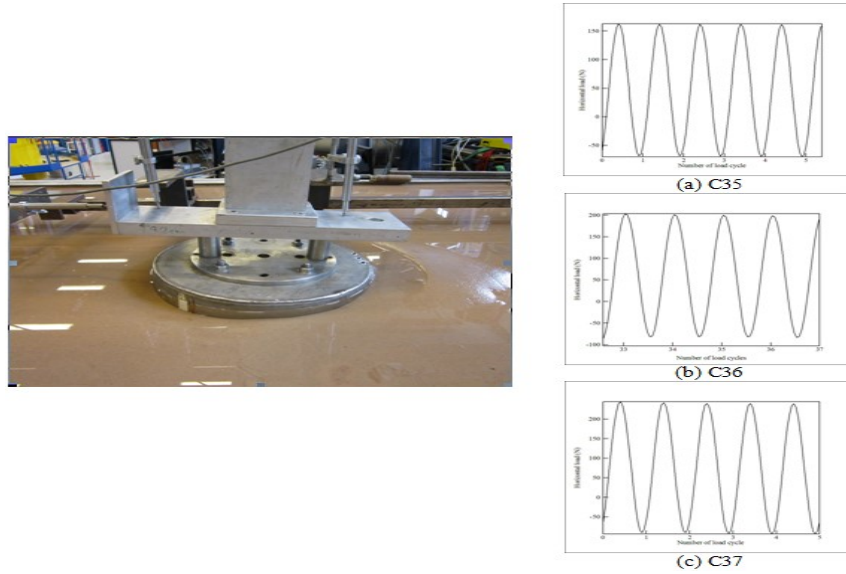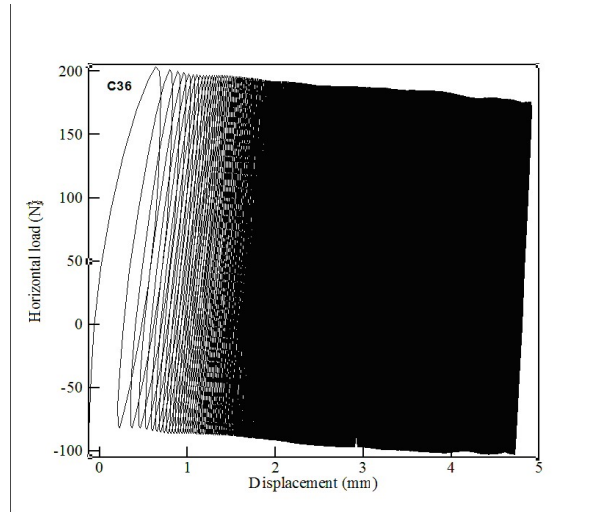

(a) C35

(b) C36

(c) C37

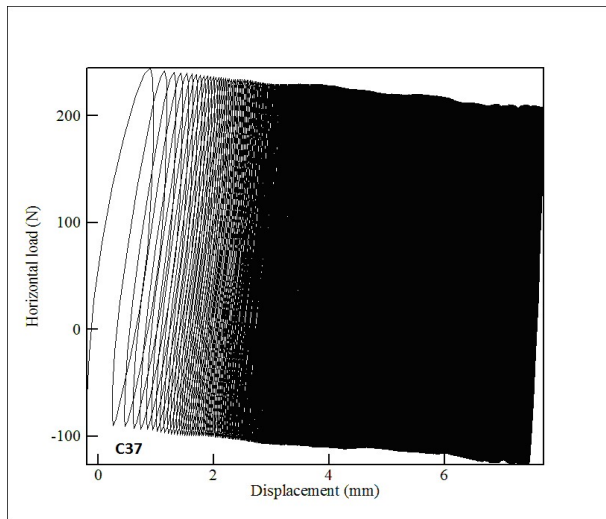**FIG. 7. Photo of experimental set-up and load-time histories of three tests a)C35 b)C36 C)37**
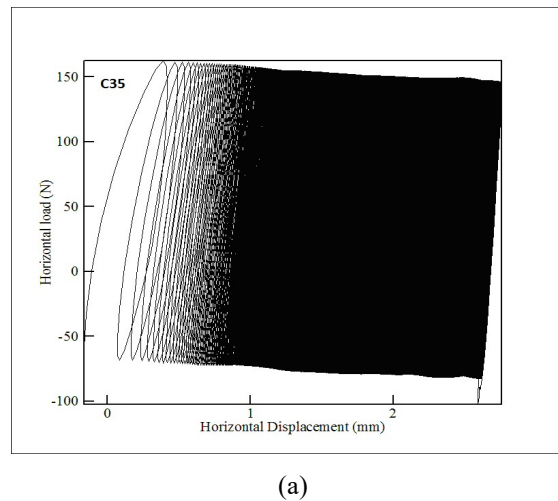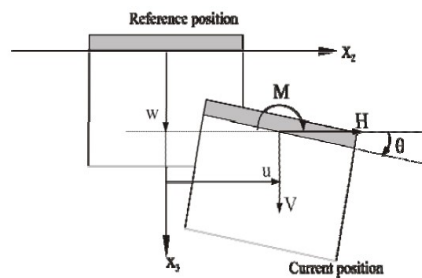

(a)

(b)

(c)

FIG. 8. The load-displacement response at load reference point during cyclic lateral load tests a) C35 b) C36 c)C37

FIG. 9. Standardized sign convention for plane loading of bucket foundations

(Butterfield et al. 1997).

**Table 2. Information on cyclic lateral load tests**

Test	Min. Force	Max. Force	ξ_b	ξ_c	Number of cycles
	N	N			
C35	-68.11	162.4	0.48	-0.54	9976
C36	-81.7	203.3	0.58	-0.56	10153
C37	-90.3	244.4	0.69	-0.58	10083

In a closer inspection, the final unloading in C35 test from ⊔ 160 N to ⊔ -70 N created a recoil of ⊔ 2.6 mm prior to stopping the rig. When C36 was subsequently carried out at ⊔ 200 N to ⊔ -80N, it may be seen that the first reloading induced ⊔ 0.4 mm, confirming that the stop-start cycle has influence on the results. However, lateral cycles with amplitude ⊔ 200 N in C36 can be seen stiffer than C35 with in increasing permanent displacement. In later test, C37, the same phenomenon occurred but very much reduced "first cycle offset".

Three performance measure parameters are introduced herein to evaluate the response of soil-foundation system.

Performance measure parameters

Figure 10 depicts secant stiffness at each unloading-reloading reversal point. The non-dimensional form of secant stiffness obtained at each unloading–reloading reversal point and the sequential reversal points, respectively divided by corresponding stiffness at first cycle is outlined in Figure 11. They are defined here as the ratio of the lateral load to the reference point lateral displacement at the soil-foundation interaction. After a tremendous increase in the first cycle, the ⊔ $K_{s,n}$ increases slightly with the increasing number of load cycles but at a reducing rate, as shown in Figure 11. The increase in the measured stiffness may be attributed to the soil densification during cyclic loading. It is worthy of note that the roughly nonlinear behavior during the tests causes a gradual increase in $K_{s,n}$. Given that the amplitude of cyclic loads was big enough to trigger the soil hardening, the largest value of $K_{s,n}$ in all tests is about 1694 N/mm after cyclic loading.
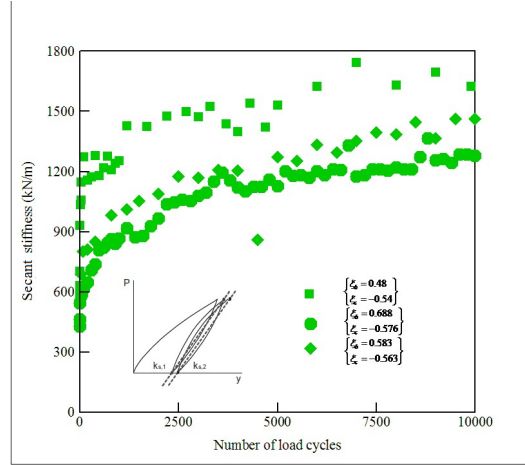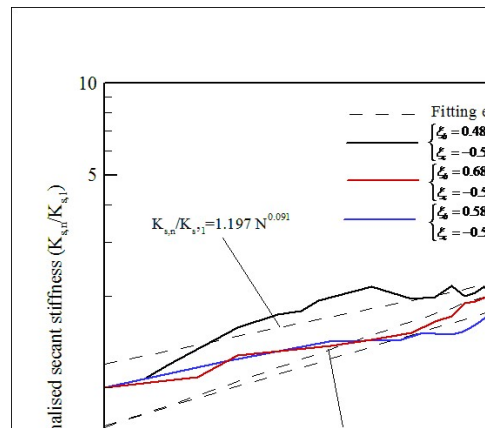
FIG. 10. Bucket secant lateral stiffness

Plotting non-dimensional secant stiffness as a function of N^b suggests that stiffness evolves exponentially with cycle number as:

$$k = \frac{K_{s,n}}{K_{s,1}} = aN^b \qquad (3)$$

where *a* and *b* are correlation coefficients. The expression in Eq. (4) was fitted to the data in Figure 11 and the *a* was determined as a function of load characteristics. It is observed from Figure 11 that all power values are almost equal. It implies that *b* is independent of the load characteristics within the observed range. This issue is further examined in a later publication in terms of wide range of forcing excitations.

FIG. 11. Normalized bucket secant lateral stiffness

The stability of the soil-foundation system for lateral response of buckets in sand is further investigated through analysis of accumulation rate of plastic displacement. Figure 12 presents the relative bucket head displacement between two subsequent re-loading un-loading reversal points normalized with the one between virgin loading-

unloading and the first reloading -unloading reversal points. Typical results from test C36 shows that rate of accumulation of plastic displacement decreased as the number of load cycles increased, indicative of the stable response of the system.
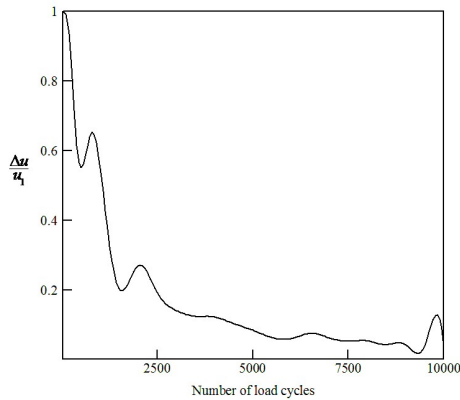
FIG. 12. Relative bucket head displacement between two consecutive re-loading unloading reversal points normalized with the one between the virgin loading and the first re-loading unloading reversal point

CONCLUSIONS

This paper has presented selected results from finite element simulations and laboratory testing program aimed at investigating the response of suction caisson foundations to combined loads in terms of performance measure parameters.

The force-controlled cyclic loads induced significant accumulated displacements that may be attributed to the local densification of sand in soil-foundation interface. Considering the dramatic increase in bucket lateral secant cyclic stiffness in the first cycle, stiffness increases slightly with the increasing number of load cycles but at a reducing rate. The $K_{s,n}$ values rise by around 2.8 times irrespective of the load amplitude.

Finally, the paper described in outline a theoretical framework that captures the main features of the cyclic tests- that of clear trend of hardening response, practically affected by the load path. This new soil-foundation interaction model termed performance based design model, represents a significant improvement on conventional theories, which could not capture this behavior.

REFERENCES

Achmus M. *et al*. (2013). Load-bearing behavior of suction bucket foundations in sand. Applied Ocean Research, 43, 157-165.

API. (1993). Recommended practice for planning, designing, and constructing fixed offshore platforms: working stress design. 20th edn. Washington, D.C: American Petroleum Institute; RP2A-WSD.

Arany L. *et al*. (2017). Design of monopiles for offshore wind turbines in 10 steps. Soil Dynamics and Earthquake Engineering, 92, 126-152.

Bhattacharya S. and Adhikari, S. (2011). Experimental validation of soil–structure interaction of offshore wind turbines. Soil Dynamics and Earthquake Engineering, 31, 805–816.

Barari A. and Ibsen L.B. (2014). Vertical capacity of Bucket foundations in undrained soil. Journal of Civil Engineering and Management, 20(3), 360-371.

Barari A. and Ibsen L.B. (2012). Undrained response of Bucket foundations to moment loading. Applied Ocean Research, 36, 12-21.

Butterfield R. *et al*. (1997). Standardized sign conventions and notation for generally loaded foundations. Geotechnique, 47(5), 1051–1054.

Cox J. et al. (2011). "Long term performance of suction caisson supported offshore wind turbines. The Structural Engineer., 89(19), 12–13.

Doherty P. and Gavin K. (2012). Cyclic and rapid axial load tests on displacement piles in soft clay. Journal of Geotechnical and Geoenvironmental Engineering, 138(8), 1022-1026.

EAU. (2004). Empfehlungen des Arbeitsausschusses "Ufereinfassungen" – Häfen und Wasserstraßen. Verlag Ernst & Sohn, Berlin.

Foglia A. *et al*. (2012). Physical modelling of Bucket foundation under long-term cyclic lateral loading. Proc. of the International Offshore and Polar Engineering Conference, Rhodos, 667-673.

Gerolymos N. *et al*. 2012. Insight to failure mechanisms of caisson foundations under combined loading: A Macro-Element Approach. Second International Conference on Performance-Based Design in Earthquake Geotechnical Engineering, Taormina, Italy.

Ibsen L.B. *et al*. (2014a). An adaptive plasticity model for Bucket foundations. Journal of Engineering Mechanics, ASCE, 140, 361–373.

Ibsen L.B. *et al*. (2014b). Calibration of failure criteria for Bucket foundations under general loading. Journal of Geotechnical and Geoenvironmental Engineering, ASCE, DOI: 10.1061/(ASCE)GT.1943-5606.0000995.

Ibsen L.B. *et al*. (2015). Effect of embedment on the plastic behaviour of Bucket Foundations. Journal of Waterway, Port, Coastal, and Ocean Engineering, ASCE, DOI: 10.1061/(ASCE)WW.1943-5460.0000284, 06015005.

Jardine, R.J. and Standing J.R. (2012). Field axial cyclic loading experiments on piles driven in sand. Soils and Foundations, 52(4), 723–736.

Kuo Y.S. *et al.* (2012).Minimum embedded length of cyclic horizontally loaded monopiles, Journal of Geotechnical and Geoenvironmental Engineering, 138, 357-363.

Larsen K.A. *et al*. (2013). Modified expression for the failure criterion of Bucket foundations subjected to combined loading. Canadian Geotechnical Journal, 50(12), 1250-1259.

Roscoe K. H. and Schofield A. N. (1957). The stability of short pier foundations in sand. British Welding Journal, January, 12-18.